GSA DATA REPOSITORY 2012027

Discovery of a Carnian (Late Triassic) negative $\delta^{13}C$ spike linked to the eruption of Wrangellia flood basalts

Jacopo Dal Corso[1], Paolo Mietto[1], Robert J. Newton[2], Richard D. Pancost[3], Nereo Preto[1], Guido Roghi, Paul B. Wignall[2]

[1]Dipartimento di Geoscienze, Università degli Studi di Padova, via Gradenigo 6, 35131 Padova, Italy

[2]School of Earth and Environment, University of Leeds, Woodhouse Lane, Leeds, LS2 1JT, UK

[3]Organic Geochemistry Unit, Bristol Biogeochemistry Research Centre, School of Chemistry, The Cabot Institute, University of Bristol, Bristol BS8 1TS, UK

[4]Istituto di Geoscienze e Georisorse, CNR, via Gradenigo 6, 35131 Padova, Italy

STUDY AREA

A map of the study area is given in Figure DR1.

MATERIALS AND METHODS

Compound Specific Isotope Analysis

Rocks were cleaned with methanol and then ground using a pestle and mortar. The sediments were extracted by using dichloromethane and methanol (DCM:MeOH 2:1 v/v) in a Soxhlet apparatus. The total lipid extract was separated into neutral fraction using dichloromethane/*iso*-propanol (DCM/iPA 2:1 v/v) and acid fraction using aminopropyl solid phase extraction columns with MeOH and 2% acetic acid in ether. Neutral fractions were further separated into apolar (hexane/DCM 9:1 v/v) and polar (DCM/MeOH 1:2 v/v) fractions using alumina flash column chromatography.

Compounds $\delta^{13}C$ was analyzed in duplicate (σ = 0.1 to 1.8, see Table DR1) using an Agilent 6890 gas cromatographer coupled with a Finnigan MAT Delta^{PLUS}XL isotope ratio mass spectrometer (GC-IRMS). Separation of compounds was achieved using a Non Polar column HP1 (50 m x 0.32 mm internal diameter). GC oven temperature was programmed from 70° C to 130° C at a rate of 20° C/min, then from 130° C to 300° C (rate: 4° C/min) and finally hold at 300° C for 25 min.

A characteristic chromatogram of the extracted apolar fraction is given in Figure DR2.

$\delta^{13}C$ of wood and TOC

$\delta^{13}C_{org}$ analyses were performed on a Micromass Isoprime continuous flow mass spectrometer coupled to a Eurovector Elemental Analyser. Rock and wood powders were acid washed in ~1.2 M HCl overnight, before washing in distilled water and drying. The resulting powders were weighed into tin cups. Organic carbon was quantitatively converted to CO_2 by flash combustion at 1020°C in the presence of pure O injected into a stream of He. Excess O was removed by reaction with hot copper wires at 650°C, water was removed in a magnesium

perchlorate trap and the CO_2 separated from other impurities using a chromatographic column. $^{12}C/^{13}C$ is derived from the integrated mass 44, 45 and 46 signals from the pulse of sample CO_2, compared to those in an independently introduced pulse of CO_2 reference gas. These ratios are calibrated using international standards ANU-sucrose (-10.47‰) and IAEA-CH7 (polyethylene film, -31.83‰). The precision obtained for repeat analysis was better than ± 0.2‰ (σ). See Table DR2 and Table DR3 for a complete list of all TOC and wood C-isotopic data.

Palynomorphs extraction

Portions of the same samples analyzed for CSIA have been grounded and treated with HCl and HF. After washing and sieving (15 μm), the residue has been stored in deionized water.

Carbon Preference Index

The carbon preference index (CPI) was calculated for *n*-C_{25} – *n*-C_{31} n-alkanes following the equation:

$$CPI = [((C_{25}+C_{27}+C_{29})/(C_{26}+C_{28}+C_{30}))+((C_{27}+C_{29}+C_{31})/(C_{26}+C_{28}+C_{30}))]/2$$

Extracted HMW n-alkanes from Stuores-Wiesen and Milieres-Dibona sections show CPIs from 1.5 to 2.3 (Tab. DR1). Modern higher plants generally show a strong odd-over-even carbon number predominance and CPI values higher than 4. CPI values lower than 4 would suggest microbial or algal contribution to long chained n-alkanes, or degradation of organic matter (Pancost and Boot, 2004). Moreover, Lichtfouse et al. (1999) have demonstrated that freshwater algae *Botriococcus braunii* have an HMW n-alkanes distribution very similar to higher plant HMW n-alkanes.

Preliminary qualitative palynological analyses of samples analyzed for CSIA show that *Botryococcus* is not present or very rare, excluding its contribution to the HMW n-alkanes.

Here reported CPI values (Table DR1) are very similar to those calculated for end-Triassic leaf-waxes n-alkanes extracted from sediments deposited in a similar environmental setting (Ruhl et al., 2011) and generally higher than those calculated for end-Triassic – early-Jurassic leaf-waxes n-alkanes from Hartford-Newark and St. Audrie's Bay sections (Whiteside et al., 2010). This fact suggests that Carnian CPI values are consistent with other Late Triassic CPIs of higher plant leaf-waxes n-alkanes.

Furthermore, GC-MS data (not shown here) show that n-alkanes extracted from microbial carbonates from the same studied sections have a completely differet distribution with a relative abundance of HMW n-alkanes lower than mid-low molecular weigh n-alkanes and no odd-over-even carbon number predominance (CPI values closely around 1), excluding any microbial or algal origin for shales' HMW n-alkanes extracted.

Thus, HMW n-alkanes from Stuores-Wiesen and Milieres-Dibona sections are reasonably thought to derive from higher plant leaf-waxes and therefore their C-isotopic composition represent the atmospheric $\delta^{13}C$.

AGE OF WRANGELLIA LIP

In different Wrangellia outcrops in Alaska and Canada (Greene et al., 2010) silicified shales, black shales, chert and limestones underlying Wrangellia basalts contain Ladinian bivalves

belonging to the genus *Daonella* (Greene et al., 2010) and overlying sediments, mainly limestones, present a lower Tuvalian (upper Carnian) ammonoid association with *Tropites dilleri* (Tozer, 1994). Most of the existing absolute Ar/Ar ages of Wrangellia basalts are reset to ages younger than that of deposition (Greene et al., 2010 and references therein). However, some U/Pb ages of multigrain zircon fractions and multigrain baddeleyite fraction (Greene et al., 2010 and references therein) are consistent with biostratigraphic constrains of Wrangellia basalts according to the most recent integrated chronostratigraphic Time Scale (Walker and Geissman, 2009) and are very similar to the existing radioisotopic minimum age for the CPE (Furin et al., 2006).

REFERENCES

Furin, S., Preto, N., Rigo, M., Roghi, G., Gianolla, P., Crowley, J.L., Bowring, S.A., 2006: High precision U-Pb zircon age from the Triassic of Italy: Implications for the Triassic time scale and the Cernian origin of calcareous nannoplankton and dinosaurs. Geology, v. 34, p. 1009-1012.

Greene, A.R, Scoates, J.S., Weis, D., Katvala, E.C., Israel, S., Nixon, G.T., 2010, The architecture of oceanic plateaus revealed by the volcanic stratigraphy of the accreted Wrangellia oceanic plateau: Geosphere, v. 6, p. 47-73.

Lichtfouse, E., Derenne, S., Mariotti, A., Largeau, C., 1999. Possible algal origin of long chain odd n-alkanes in immature sediments as revealed by distribution and carbon isotope ratios. Organic Geochemistry, v. 22, p. 1023-1027.

Pancost, R.D., and Boot, 2004. The palaeoclimatic utility of terrestrial biomarkers in marine sediments. Marine Chemistry, v. 92, p. 239-261.

Ruhl, M., Bonis, N.R., Reichard, G., Sinninghe Damsté, J.S., Kürschner, W.M., 2011. Atmospheric Carbon Injection Linked to End-Triassic Mass Extinction. Science, v. 333, p. 430-434.

Tozer E.T., 1994. Canadian Triassic Ammonoid Faunas: GSC Bulletin, v. 467.

Walker, J.D. and Geissman, J.W., 2009. Geologic Time Scale: Geological Society of America, doi: 10.1130/2009.CTS004R2C.

Whiteside, J.H., Olsen, P.E., Eglinton, T., Brookfield, M.E., Sambrotto, R.N., 2010. Compound-specific carbon isotopes from Earth's largest flood basalt eruptions directly linked to the end-Triassic mass extinction. Proceeding of the National Academy of Science, v. 107, p. 6721-6725.

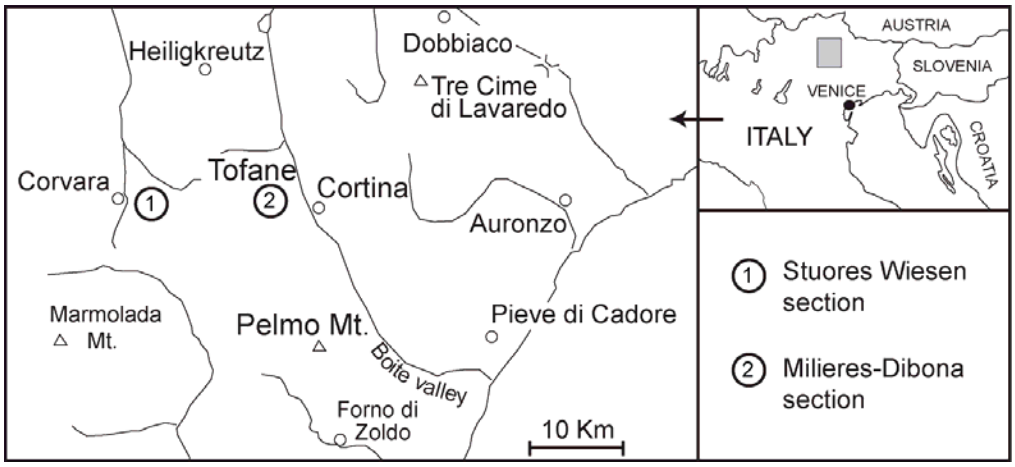

Figure DR1. Map of the study area.

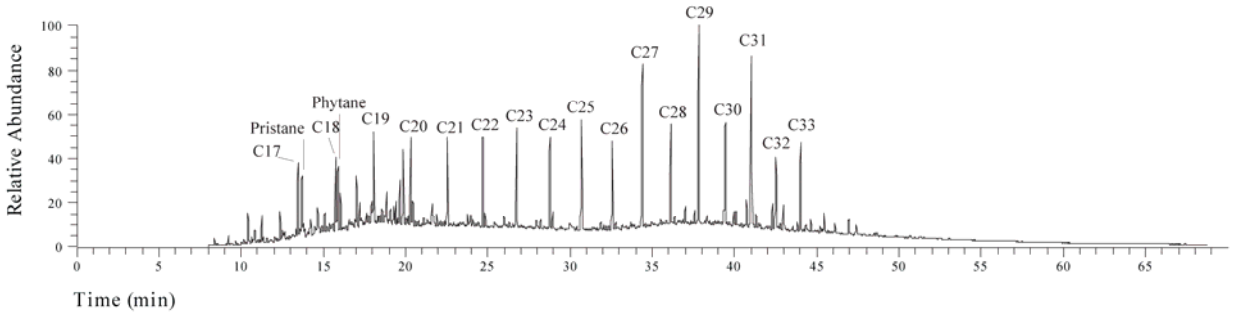

Figure DR2. Characteristic chromatogram (Total Ion Current, TIC) of extracted apolar fraction (Sample DJ16). Identified n-alkanes (C_{17} – C_{33}) and isoprenoid lipids (pristane and phytane) peaks are marked.

Table DR1. Compound Specific C-Isotope data (‰^{13}C value ± standard deviation based on duplicate analyses)

Sample	δ^{13}C n-alkane						δ^{13}C isoprenoid		CPI
	C_{17}	C_{19}	C_{25}	C_{27}	C_{29}	C_{31}	Pristane	Phytane	
STU 00			-26.4±0.9	-26.9±0.1	-25.7±0.2	-27±0.5			1.6
STU 5			-28±0.1	-27.9±1.5	-27.3±0.3	-25.9±0.8			1.7
STU 105			-26.4±0.8	-25.9±0	-26.7±0.5	-27.6±0.6			1.5
STU 108			-26.4±0.2	-25.5±0.1	-26.4±0.1	-26.5±0.0			1.8
MIR 1	-27.1±0.1	-26.4±0.1	-25.4±0.4	-26.6±0.6	-26.8±1.1	-23.7±0.7		-29.3	1.8
MIR 5	-32.5±0.6	-30±1.8	-30.1±0.7	-29.6±0.0	-30		-32.3	-31.6±1.5	1.8
MIR 7	-30.7±0.2	-30.2±0.5	-29.4±0.1	-30.3±0.1	-30.9±0.1	-29.5±0.8	-33.5±0.5	-30.6±1.4	1.7
MIR 9	-27.2±0.6	-26.7±0.8	-26.7±0.6	-26.2±0.3	-28.4±0.2	-26.9±0.1	-27.5±0.2	-29.9	1.7
MIR 16		-25.7±0.4	-25.4±0.3	-25.3±0.1	-26.4±0.6	-24.7±0.9	-25.8±0.1		1.6
DJ 16			-24.7±0.7	-22.9±0.4	-24.4±0.0	-25.1±0.1			2
DJ 18			-24.1±0.8	-24.3±0.9	-25.3±0.1	-24.1±0.9			2
DJ 19			-23.5±0.7	-22±0.2	-23.7±0.6	-24.1±0.3			2.3
DJ 21			-23.5±0.3	-22.5±0.2	-23.3±0.1	-23.3±0.0			1.9

Table DR2. Total Organic Carbon (TOC) C-isotope data

Sample	$\delta^{13}C_{TOC}$	meter
Stuores-Wiesen section		
STU-00-b	-24.9	19
STU-5	-24.9	41
STU-12-b	-25.5	54
STU-102	-24.8	78
STU-108-b	-23.8	124
Milieres-Dibona section		
MIR-100	-22.8	0.22
MIR-1	-22.9	0.45
MIR-101	-23	0.62
MIR-102	-22.9	1.52
MIR-103	-23.4	2.62
MIR-2	-23.4	2.9
MIR-104	-23.8	3.56
MIR-105	-23.8	5.54
MIR-106	-24.3	5.92
MIR-107	-24	7.6
MIR-108	-24.6	9
MIR-5	-24.2	14.3
MIR-109	-24.2	14.62
MIR-110	-23.9	15.3
MIR-111	-24	16.36
MIR-112	-24.5	16.96
MIR-113	-24	17.84
MIR-114	-24.1	19.12
MIR-115	-24	19.74
MIR-116	-24	19.88
MIR-117	-23.9	20.06

MIR-6	-24.5	20.12
MIR-118	-24.4	20.22
MIR-119	-24.3	20.42
MIR-120	-24.2	20.8
MIR-7	-24.4	21.08
MIR-121	-24.3	21.12
MIR-123	-24.1	21.84
MIR-124	-24.1	22.24
MIR-125	-23.9	22.6
MIR-126	-24.2	22.98
MIR-127	-24.3	23.12
MIR-128	-24.2	23.68
MIR-129	-23.5	24.16
MIR-130	-23.8	24.66
MIR-131	-23	25.74
MIR-9	-23	26
MIR-132	-23	26.08
MIR-133	-23.1	26.44
MIR-134	-22.9	27.02
MIR-135	-23.4	29.34
MIR-136	-23	30.16
MIR-10	-23.2	30.48
MIR-137	-23	30.9
MIR-138	-22.6	31.22
MIR-139	-22.4	31.54
MIR-11	-23	31.76
MIR-140	-22.8	32.02
MIR-141	-23.6	32.32
MIR-142	-23.1	33.86
MIR-143	-22.8	34.02
MIR-144	-23.6	34.24
MIR-145	-23.1	34.96
MIR-13	-23.4	35
MIR-146	-23.4	35.64
MIR-147	-23.8	36.3
MIR-148	-22.8	40.2
MIR-149	-22.8	40.58
MIR-150	-22.8	41
MIR-151	-22.7	41.4
MIR-16	-22.8	41.64
MIR-152	-23.1	41.86
MIR-153	-22.8	42.2
MIR-154	-23.1	42.56
MIR-155	-23.5	43.54
DJ-16	-22	126.93
DJ-18-b	-22.5	128.15
DJ-19-b	-22.3	129
DJ-21-b	-21.7	129.77
DJ-27-b	-22	136.69

Table DR3. Wood C-isotope data

Sample	$\delta^{13}C$	meter
Stuores-Wiesen section		
STU00	-24.93	19
STU02-4	-24.36	21
STU02-5	-23.46	21
STU02-6	-24.48	21
STU02-3D	-23.62	21
STU02-1A	-23.74	21
STU02-2B	-23.64	21
STU02-2C	-23.6	21
STU104-21	-24.76	87
STU104-23A	-24.12	87
STU104-16	-24.58	87
STU104-2	-23.95	87
STU104-8	-24.77	87
STU104-9	-23.81	87
STU104-23B	-24.39	87
STU104-5	-24.77	87
STU104-12	-23.56	87
STU104-14A	-24.15	87
STU104-10	-25.44	87
STU104-11	-23.62	87
STU104-15A	-24.98	87
STU104-15B	-24.97	87
STU104-14B	-23.7	87
STU104-15	-24.8	87
STU105	-23.12	91
STU107-6	-23.57	118
STU107-7	-23.68	118
STU107-5	-24.05	118
STU107-1	-23.6	118
STU107-3	-25.46	118
STU108-2	-25.03	124
STU108N	-23.91	124
STU108	-24.37	124
STU108-1	-24.08	124
STU108A	-23.49	154
Milieres-Dibona section		
DJ4-12	-20.96	53
DJ4-2	-21.12	53
DJ4-1	-22.25	53
DJ4-11	-21.03	53
DJ4-5	-22.02	53
DJ4-8	-23.34	53
DJ4-3	-22.55	53
DJ4-4	-21.37	53
DJ5B-3	-23.43	54
DJ5B-2	-23.23	54
DJ5B-1	-22.36	54
DJ5B-6	-23.09	54
DJ5B-7	-22.71	54

DJ5B-4	-23.14	54
DJ5B-5	-22.93	54
DJ6-5	-22.75	54.5
DJ6-6	-22.36	54.5
DJ6-7	-21.62	54.5
DJ6-4	-21.57	54.5
DJ6	-21.6	54.5
DJ6-2	-23.09	54.5
DJ6-3	-21.39	54.5
DJ5-1	-21.65	56
DJ5-10	-22.13	56
DJ5-6	-21.41	56
DJ5-4	-20.93	56
DJ5-9	-21.78	56
DJ5-8	-22.46	56
DJ5-3	-21.74	56
DJ5-12	-21.6	56
DJ5-11	-21.22	56
DJ5-2	-21.76	56
DJ5-13	-21.95	56
DJ7-13	-20.55	100.9
DJ7-14	-21.76	100.9
DJ7-2	-21.52	100.9
DJ7-1	-22.42	100.9
DJ7-11	-22.16	100.9
DJ7-12	-21.56	100.9
DJ7-3	-21.94	100.9
DJ7-7	-20.93	100.9
DJ7-8	-21.54	100.9
DJ7-9	-21.61	100.9
DJ7-4	-22.16	100.9
DJ7-5	-21.04	100.9
DJ7-6	-21.43	100.9
DJ8-1	-21.673	110.27
DJ9-11	-21.76	113.4
DJ9-12	-21.81	113.4
DJ9-1	-21.7	113.4
DJ9-10	-21.06	113.4
DJ9-14	-22.09	113.4
DJ9-5	-21.88	113.4
DJ9-9	-22.4	113.4
DJ9-4	-20.69	113.4
DJ9-2	-21.25	113.4
DJ9-3	-21.71	113.4
DJ12-13-9	-22.85	117.27
DJ12-13-15	-21.82	117.27
DJ12-8-5	-22.8	117.27
DJ12-3-4	-23.39	117.27
DJ12-1-13	-22.62	117.27
DJ12-1-10	-22.77	117.27
DJ12-12-16	-22.31	117.27
DJ12-11-7	-21.74	117.27
DJ13-4	-23.07	120.13
DJ13-3	-23.11	120.13
DJ13-6	-22.64	120.13

DJ13-5	-23.42	120.13
DJ13-10	-23.21	120.13
DJ13-1	-23.05	120.13
DJ13-12	-22.6	120.13
DJ13-11	-23.37	120.13
DJ13-9	-23.7	120.13
DJ13-8	-23.44	120.13
DJ13-7	-23.27	120.13
DJ14-6	-22.62	120.98
DJ14-5	-22.6	120.98
DJ14-8	-21.9	120.98
DJ14-7	-22.68	120.98
DJ14-3	-22.25	120.98
DJ14-10	-21.3	120.98
DJ14-1	-22.6	120.98
DJ14-2	-22.35	120.98
DJ14-11	-21.37	120.98
DJ15-12	-22.77	126.09
DJ15-11	-20.99	126.09
DJ15-10	-23.67	126.09
DJ20-5	-20.9	129.1
DJ20-6	-21.05	129.1
DJ20-7	-21.8	129.1
DJ20-4	-20.75	129.1
DJ20-10	-21.15	129.1
DJ20-2	-20.89	129.1
DJ20-3	-21.29	129.1
DJ20-8	-20.32	129.1
DJ20-1	-21.08	129.1
DJ20-9	-21.1	129.1
DJ22-4	-21.81	131
DJ22-5	-21.65	131
DJ22-1	-21.75	131
DJ22-2	-20.87	131
DJ22-3	-21.58	131
DJ23-1	-21.64	132.9
DJ24-3	-21.27	134.15
DJ24-2	-21.89	134.15
DJ26-2	-20.42	136
DJ26-1	-20.15	136
DJ28-4	-22.43	138.52
DJ28-3	-21.4	138.52
DJ28-1	-20.9	138.52
DJ29-2	-22.08	139.4
DJ29-1	-23.52	139.4